Front. Phys. 10(5), 106102 (2015)
DOI 10.1007/s11467-015-0511-z

RESEARCH ARTICLE

Unprecedentedly rapid transport of single-file rolling water molecules

Tong Qiu (邱桐)*, Ji-Ping Huang (黄吉平)†

Department of Physics, State Key Laboratory of Surface Physics, and Collaborative Innovation Center of Advanced Microstructures, Fudan University, Shanghai 200433, China

*Corresponding authors. E-mail: *qiut10@fudan.edu.cn, †jphuang@fudan.edu.cn*

Received June 1, 2015; accepted August 24, 2015

The realization of rapid and unidirectional single-file water-molecule flow in nanochannels has posed a challenge to date. Here, we report unprecedentedly rapid unidirectional single-file water-molecule flow under a translational terahertz electric field, which is obtained by developing a Debye double-relaxation theory. In addition, we demonstrate that all the single-file molecules undergo both stable translation and rotation, behaving like high-speed train wheels moving along a railway track. Independent molecular dynamics simulations help to confirm these theoretical results. The mechanism involves the resonant relaxation dynamics of H and O atoms. Further, an experimental demonstration is suggested and discussed. This work has implications for the design of high-efficiency nanochannels or smaller nanomachines in the field of nanotechnology, and the findings also aid in the understanding and control of water flow across biological nanochannels in biology-related research.

Keywords water molecules, carbon nanotubes, molecular dynamics, terahertz electric field, electrohydrodynamics, Debye double-relaxation theory

PACS numbers 47.61.-k, 61.20.Ja

1 Introduction

Owing to the importance of water to human life, this substance has attracted considerable attention from scientists in various fields, including physics, chemistry, biology, nanotechnology, and environmental science. Currently, the study of water flow across nanochannels is an important topic. Its significance is at least two-fold, as this behavior has implications for seawater desalination or water purification by using filtering methods [1–5] and it is also of importance as regards the understanding and control of water flow across water nanochannels in biological membranes [1, 6–10]. In both of these cases, achievement of a fast unidirectional flow of single-file water molecules across nanochannels has posed a significant challenge to date. For this purpose, nanochannels such as carbon nanotubes are often used for water transportation because of their (almost) frictionless interfaces [1, 8, 9, 11–16]. Accordingly, researchers have developed and studied many new techniques for transporting water through nanochannels, e.g., diffusion osmosis, pressure differences, thermal gradients, channel deformation, and radial breathing mode vibrations [17–21]. In particular, electrical methods have been widely used to generate unidirectional water flow. For instance, researchers have designed various types of electric fields using linear gradient fields, rotating fields, or electrostatic charges [9, 10, 22–28].

Because of these efforts, the maximum (linear) transport speed of water molecules in nanochannels has increased significantly (e.g., refs. [1, 7, 14, 21, 22, 25, 27, 29]), which encourages exploration of new approaches to this topic. Moreover, it is well known that the function of charge groups in biological membrane proteins is vital to water permeation through aquaporins [30–34] (*biological implication*). For instance, asparagine-proline-alanine regions in both aquaporin-1 and glycerol uptake facilitator proteins and mediate the action of a selective water filter [33, 34]. On the other hand, environmental oscillations arising from thermal motion occur when water molecules are transported through nanochannels [21] (*physical implication*).

In this work, we investigate a model system (see Fig.

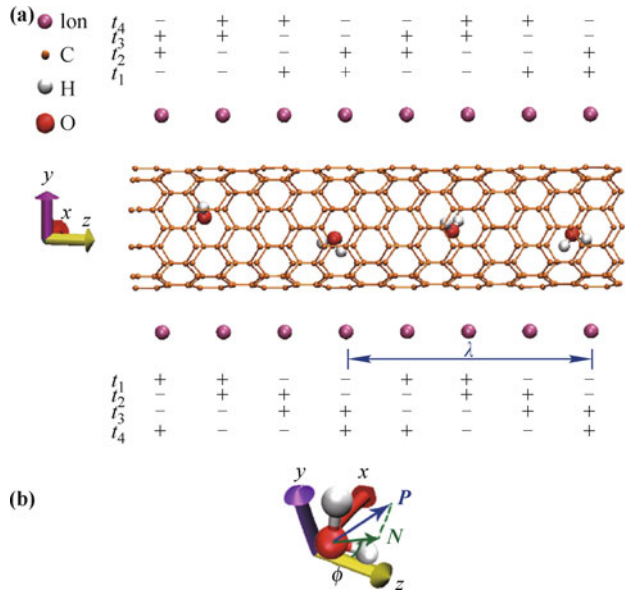

Fig. 1 **(a)** Schematic graph showing a fixed z-directed nanochannel containing single-file water molecules located between two symmetric arrays of nanoelectrodes. The charges of the fixed nanoelectrodes alternate in the way of a periodic four-time-interval (i.e., $t_1 \to t_2 \to t_3 \to t_4 \to ...$) arrangement. **(b)** Schematic graph for the definition ϕ of a water molecule (with permanent dipole moment vector $\boldsymbol{P}$); $\boldsymbol{N}$ is the projection of $\boldsymbol{P}$ on the yz plane.

1) that is inspired by these biological and physical implications. Hence, we determine that single-file water molecules experience rapid transport, behaving like the wheels of a high-speed train moving along a railway. Therefore, we label this type of transport a *water nanotrain*. Our investigation is based on a phenomenological Debye double-relaxation theory together with independent molecular dynamics simulations.

2 Debye double-relaxation theory

Let us begin by considering an isolated water molecule at room temperature. It is known that the spontaneous polarizability of the water molecule can be characterized by a permanent dipole moment $\boldsymbol{P}$. Then, an external electric field $\boldsymbol{E}$ with angular frequency ω can be added to the water molecule. In this case, if $\boldsymbol{E} \to 0$, p, which denotes the average $\boldsymbol{E}$-direction projection of $\boldsymbol{P}$, is sufficiently small, because of the irregular thermal motion of the molecule. Hence, for $\boldsymbol{E} \to 0$, we obtain $p \to 0$. Certainly, owing to the competition between thermal motion (which tends to cause irregular molecular motion) and $\boldsymbol{E}$ (which tends to direct the molecule in the $\boldsymbol{E}$ direction), an increasing $\boldsymbol{E}$ causes p to increase up to $p = |\boldsymbol{P}|$. Thus, p depends on the strength of $\boldsymbol{E}$, which allows us to regard p as an *effectively* induced dipole moment. Next, we model the water molecule as a spherical nanoparticle with radius a, and assume that its p can be expressed in the same manner as the induced dipole moment of a spherical dielectric particle [35–39], such that

$$p = 4\pi\varepsilon_0 a^3 G(\omega) E, \tag{1}$$

where ε_0 is the vacuum permittivity and $E = |\boldsymbol{E}|$. $G(\omega)$ denotes the ω-dependent dipole factor (also called the Clausius–Mossottii factor, which characterizes the dielectric contrast between the molecule and vacuum), where

$$G(\omega) = \frac{\hat{\varepsilon}(\omega) - 1}{\hat{\varepsilon}(\omega) + 2}. \tag{2}$$

In Eq. (2), the complex permittivity $\hat{\varepsilon}(\omega)$, which describes the effective dielectric response of the water molecule to $\boldsymbol{E}$, may be formulated in terms of the Debye double-relaxation model [40–43]

$$\hat{\varepsilon}(\omega) = \varepsilon_\infty + \frac{\Delta\varepsilon_1}{1 + \mathrm{i}\omega\tau_1} + \frac{\Delta\varepsilon_2}{1 + \mathrm{i}\omega\tau_2}, \tag{3}$$

where $\mathrm{i} = \sqrt{-1}$ and ε_∞ is the permittivity at the high-frequency limit. The last two terms on the right-hand side of Eq. (3) describe the two relaxation processes, each arising from one type of atom (namely, O or H) in the molecule. In Eq. (3), $\Delta\varepsilon_1$ and $\Delta\varepsilon_2$ denote the amplitudes of the two relaxation processes with two corresponding relaxation times, τ_1 and τ_2, respectively [44]. For clarity, we set τ_1 (or τ_2) to represent the relaxation time of the O (or H) atom, thus yielding $\tau_1 > \tau_2$. Clearly, the substitution of $\boldsymbol{E} \to 0$ into Eq. (1) yields $p \to 0$, which echoes the preceding requirement. In addition, as the strength of the permanent dipole moment of a water molecule has a known value of 1.85 D, this value can be used to estimate the maximum strength of $\boldsymbol{E}$. This validates Eq. (1).

As mentioned in the preceding section, the primary aim of this work is to achieve a fast unidirectional water-molecule flow through a nanochannel. For this purpose, we attempt to apply a translational electric field generated by two symmetric nanoelectrode arrays, as shown in Fig. 1(a). The fixed nanoelectrodes align on both sides of the nanochannel, and their charges vary according to a periodic arrangement comprising four time intervals (i.e., $t_1 \to t_2 \to t_3 \to t_4 \to ...$). The + and − symbols denote positive and negative electric charges, respectively. The field shown in the figure is defined as being in the positive direction, because each pair of adjacent charges with the same sign (positive or negative) on either side skips in the positive z direction. Note that we utilize a nanoelectrode design that is in accordance with the microelectrode arrangement used in experiments on traveling electric fields. These arrangements are used to transfer dielectric particles (e.g., yeast cells) [45–48]. To proceed, we set the water molecule density to a low value so that

the interactions between the molecules can be neglected.

According to the charge arrangement depicted in Fig. 1(a), the $\boldsymbol{E} \to 0$ generated at the nanochannel central axis ($y = 0$) can be expressed as the summation of three components (E_x, E_y, and E_z along the x-, y-, and z-axes, respectively), with

$$\boldsymbol{E} = E_x\hat{\boldsymbol{x}} + E_y\hat{\boldsymbol{y}} + E_z\hat{\boldsymbol{z}}. \tag{4}$$

Here, $E_x = 0$ because of the symmetry of the structure along the x-axis. Further, E_y and E_z are expressed in the following forms in terms of time t [45]

$$E_y = A(y=0)\cos\left(\omega t - \frac{2\pi z}{\lambda}\right), \tag{5}$$

$$E_z = \frac{\lambda}{2\pi}A'(y=0)\sin\left(\omega t - \frac{2\pi z}{\lambda}\right), \tag{6}$$

where $A(y = 0) \equiv A(0)$ is the $\boldsymbol{E}$ strength determined by all the electric charges on the nanoelectrodes, and $A'(y = 0) \equiv A'(0)$ is the y-derivative of $A(0)$. In Eqs. (5)–(6), ω specifically denotes the angular frequency of the charge shifting and λ denotes the wavelength, as indicated in Fig. 1(a).

We are now in a position to derive the force $\boldsymbol{F}$ and torque $\boldsymbol{\Gamma}$ acting upon each water molecule due to $\boldsymbol{E}$, in order to obtain expressions for both the linear speed v_z and the angular speed Ω of the water molecules. For simplification, we assume that each water molecule moves along the central axis of the nanochannel. In particular, some narrow nanochannels, such as a (10, 0) carbon nanotube (the radius of which is 0.386 nm), provide a quasi-one-dimensional (1D) inner space for molecular transport. In such confinement, the net effect of the water transport can be neglected, except in the axial direction.

As the electric force $\boldsymbol{F}$ acting on an electric dipole is known to be $\boldsymbol{F} = (\boldsymbol{p}\cdot\nabla)\boldsymbol{E}$, the z-directed force component F_z for the water molecule is given by

$$\boldsymbol{F}_z = -\frac{4\pi^2\varepsilon_0 a^3}{\lambda}A(0)^2\mathrm{Im}[G(\omega)]\hat{\boldsymbol{z}}, \tag{7}$$

where $\mathrm{Im}[G(\omega)]$ (< 0) denotes the imaginary part of $G(\omega)$. Clearly, the presence of F_z helps to increase the z-directed v_z of the water molecule.

When linear transportation of the water molecule along the z-axis within the nanochannel begins, under the influence of $\boldsymbol{F}_z$, the interfacial friction between the water and the carbon nanotube induces a drag force $\boldsymbol{F}_f$ that acts on the water in the $-z$ direction. This tends to decrease the linear speed of the molecule. Because of the linear relationship between $\boldsymbol{F}_f$ and v_z [49], we make a phenomenological assumption that these terms are proportional to each other. Then, we express this assumption in Stokes' form: $\boldsymbol{F}_f = -6\pi\eta_l a v_z\hat{\boldsymbol{z}}$, where η_l is a coefficient analogous to the effective linear viscosity. When the system reaches equilibrium, i.e., $\boldsymbol{F}_z + \boldsymbol{F}_f = \boldsymbol{0}$, v_z reaches a constant value. This is defined as

$$v_z = -\frac{2\pi\varepsilon_0 a^2}{3\eta_l\lambda}A(0)^2\mathrm{Im}[G(\omega)]. \tag{8}$$

Clearly, v_z is proportional to the imaginary part of $G(\omega)$.

On the other hand, it is easy to determine that the phase of p [Eq. (1)] lags behind that of the electric field $\boldsymbol{E}$ [Eq. (4)], thus yielding a non-zero angle between p and $\boldsymbol{E}$. This angle induces a $\boldsymbol{\Gamma}$ on the water molecule, $\boldsymbol{\Gamma} = \boldsymbol{p}\times\boldsymbol{E} \equiv \Gamma_x\hat{\boldsymbol{x}} + \Gamma_y\hat{\boldsymbol{y}} + \Gamma_z\hat{\boldsymbol{z}}$, which causes the molecule to rotate. Here, both Γ_y and Γ_z are roughly zero at the central axis ($y = 0$), and

$$\Gamma_x = -\varepsilon_0\lambda a^3 A'(a)A(0)\mathrm{Im}[G(\omega)]. \tag{9}$$

Hence, we consider the Γ_x-induced rotations on the yz-plane only, i.e., the rotation of the ϕ depicted in Fig. 1(b). Here, ϕ denotes the angle between the z-axis and $\boldsymbol{N}$, which is the projection of the $\boldsymbol{P}$ of the water molecule on the yz-plane. Similar to the above analysis of $\boldsymbol{F}_f$, we assume that the magnitude of the drag torque $\boldsymbol{\Gamma}_d$ acting on the water molecule is proportional to Ω, with $\boldsymbol{\Gamma}_d = -8\pi\eta_r a^3\boldsymbol{\Omega}$, also in Stokes' form. Here, η_r is a coefficient analogous to the effective rotational viscosity. Like $\boldsymbol{F}_f$, $\boldsymbol{\Gamma}_d$ also arises from the interfacial friction between the water and the nanotube. In balance between $\boldsymbol{\Gamma}_x$ and $\boldsymbol{\Gamma}_d$ is achieved, Ω also reaches a constant (similar to the constant v_z discussed above), such that

$$\Omega = -\frac{\varepsilon_0\lambda}{8\pi\eta_r}A'(a)A(0)\mathrm{Im}[G(\omega)]. \tag{10}$$

Further, similar to v_z [Eq. (8)], Ω [Eq. (10)] is proportional to $\mathrm{Im}[G(\omega)]$.

In Fig. 2, $\mathrm{Im}[G(\omega)]$ is plotted for various τ_1, τ_2, $\Delta\varepsilon_1$, and $\Delta\varepsilon_2$, considering Eq. (8). Hence, it is apparent from this figure that v_z always exhibits two peaks regardless of the values of the latter four terms. From Eq. (3), we conclude that the two peaks originate from the two relaxation processes of the H and O atoms in the water molecule, respectively. Figure 2 also implies that a typical ω exists at which v_z reaches a maximum, namely, $v_{z,max}$. Thus, the parameters that determine the behavior of the two relaxation processes (namely, τ_1, τ_2, $\Delta\varepsilon_1$, and $\Delta\varepsilon_2$) have evident effects on the position and magnitude of $v_{z,max}$. In particular, τ_2 has a more prominent influence on the position of $v_{z,max}$ relative to the ω axis than τ_1. Likewise, $\Delta\varepsilon_2$ influences the magnitude of $v_{z,max}$ more strongly than $\Delta\varepsilon_1$. These results also hold for Ω as, similar to v_z, Ω is proportional to $\mathrm{Im}[G(\omega)]$ in accordance with Eq. (10). That is, the typical ω yielding $v_z = v_{z,max}$ also causes simultaneous maximum Ω

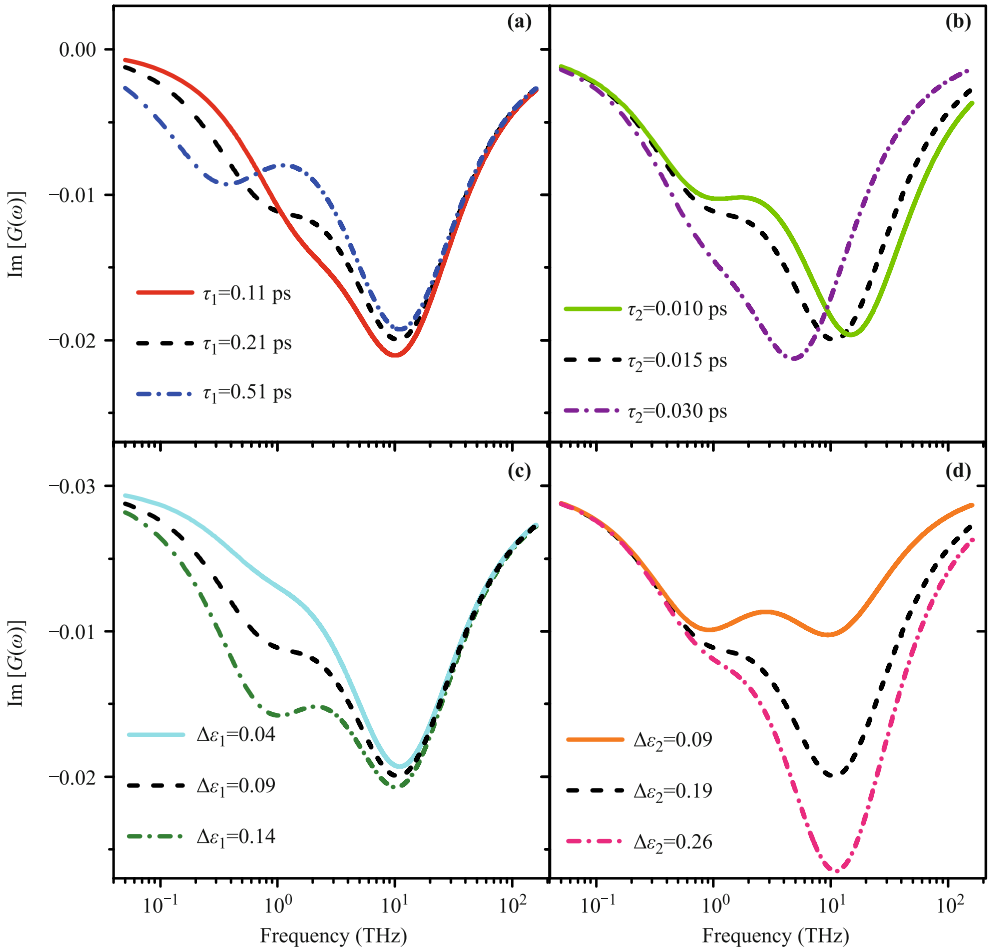

Fig. 2 Im$[G(\omega)]$ as a function of frequencies on a logarithmic scale, for different **(a)** τ_1, **(b)** τ_2, **(c)** $\Delta\varepsilon_1$, and **(d)** $\Delta\varepsilon_2$. where $\Delta\varepsilon_1$ and $\Delta\varepsilon_2$ are the amplitudes of the relaxation processes with characteristic relaxation time τ_1 and τ_2 in Eq. (3), respectively.

(Ω_{max}). This means that, when the molecule is transported along the z-axis at $v_{z,max}$, it also rotates within the yz-plane at a speed of Ω_{max}. Clearly, in this situation, all the single-file molecules behave like the wheels of a high-speed train rolling along a railway and, thus, we can refer to this type of transport as a *water nanotrain*. In fact, according to Fig. 2, this water nanotrain behavior holds over the entire frequency range.

At this stage of the discussion, the reader may question the accuracy of the water nanotrain concept, as we have made certain assumptions in order to develop this phenomenological theory. Therefore, so as to strengthen the validity of our theoretical findings, we next employ independent molecular dynamics simulations that are free from these assumptions.

3 Molecular dynamics simulations: Comparison with theory

The molecular dynamics simulations described here are performed using the Gromacs 3.3.1 [50] simulation system, which produces results such as those shown in Fig. 1(a). The nanochannel, which is a $z-$directed $(10, 0)$ single-walled carbon nanotube, has 0.386-nm radius and 9.590-nm length. All the carbon atoms are immobilized. To echo the above theoretical setting, we apply a low-density condition to the water molecules such that the initial state corresponds to scattered water molecules within the nanotube. In fact, the low-density condition eliminates interaction between the water dipoles, which would affect the responses of certain water molecules to the external fields. Thus, the directions of the water dipoles can be better mediated by the electric fields under the low-density condition. The water model used here is known as the transferable intermolecular potential three-point model [51]. Further, all atoms considered in this study obey the Lennard-Jones interaction, the parameters of which are taken from Ref. [8]. Each ion is positioned at $y = \pm 0.728$ nm [see Fig. 1(a)] and $\lambda = 1.6$ nm [as denoted in Fig. 1(a)]. We also set each ion to carry an electric charge of $5e$ or $-5e$ in our simulations. The sim-

ulation box has dimensions of $4.016 \times 4.616 \times 9.701\,\mathrm{nm}^3$, which is established using a periodic boundary condition in all three dimensions. We perform the simulations in a canonical ensemble at 300 K with a 2-fs time step.

Figure 3 displays the simulation (dots) and theory (lines) results. Note that we calculate Ω from $\Omega = |(1/t)\int_0^t \phi(t')\mathrm{d}t'|$, where $\phi(t')$ is the time-dependent angle between the z-axis and $\boldsymbol{N}$. For the theory results (lines), we adopt $\varepsilon_\infty = 1.77$, which is an approximate value to experimentally measured results [37]. Finally, $\tau_1 = 0.21$ ps and $\tau_2 = 0.015$ ps. Note that τ_1 is close to the experimental values yielded by terahertz (THz) spectroscopy studies [41, 42], and that the τ_2 we employ has the same order of magnitude as the water relaxation result yielded by the simulations [25]. The details of the comparison between simulation and theory are given below.

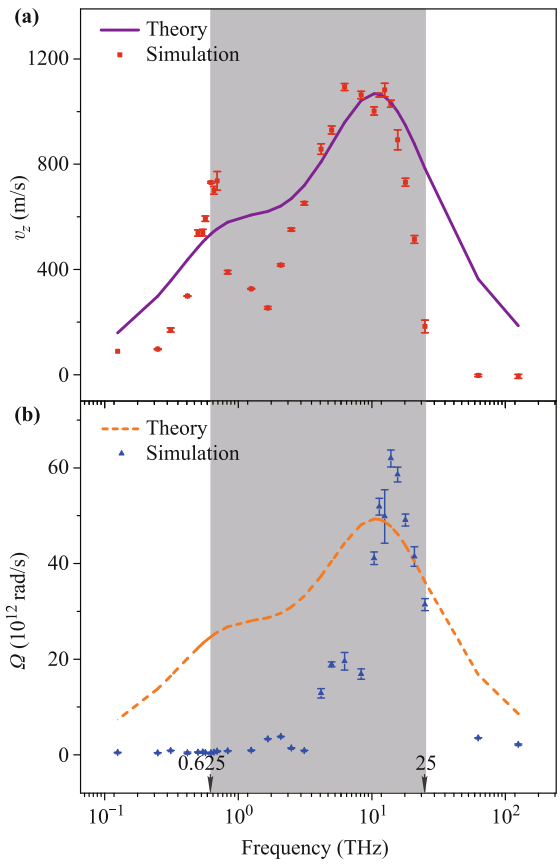

Fig. 3 Comparison between theoretical results (*lines*) and simulation data (*dots*): **(a)** Linear speed v_z and **(b)** angular speed Ω as a function of frequencies on a logarithmic scale. The solid line in (a) and dash line in (b) are obtained according to Eq. (8) and Eq. (10), respectively. We use shading to indicate the frequency range from 0.625 THz to 25 THz, which corresponds to the train-like motion of water molecules in simulations. The error bars indicated in the figure are calculated from the data of simulations for three times. Parameters for theory: $A(0) = 19.84\,\mathrm{V/nm}$, $\varepsilon_\infty = 1.77$, $\Delta\varepsilon_1 = 0.087$, $\Delta\varepsilon_2 = 0.19$, $\tau_1 = 0.21$ ps, $\tau_2 = 0.015$ ps, $\eta_l = 1.06 \times 10^{-6}\,\mathrm{kg/(ms)}$, and $\eta_r = 1.01 \times 10^{-7}\,\mathrm{kg/(ms)}$.

In Fig. 3(a), the simulated v_z displays two peaks at 0.625 and 12.5 THz, which are in accordance with the theoretical predictions. However, in Fig. 3(b), the simulated Ω exhibits only one evident peak (located at an ω value close to 12.5 THz). The disappearance of the 0.625-THz peak in the simulation results for Ω implies that the water-molecule rotation is significantly affected by Brownian motion. From a practical perspective, Brownian motion (which was not considered in the above phenomenological theory) affects Ω more significantly for an ω value of 0.625 THz than 12.5 THz. The source of this behavior may be related to the frequency of the water-molecule spontaneous oscillation [52, 53]. However, further investigation of this topic is required. In this sense, for a field with 12.5-THz frequency, changes to the field-directed orientation of a water molecule occur so rapidly that the thermal motion cannot follow. Hence, the effect of the thermal motion degrades at 12.5 THz ($\gg 1$ THz). This can explain why a peak located in the vicinity of 12.5 THz can be obtained through our simulations [see Fig. 3(b)], in agreement with the peak obtained at the same position in the theoretical results. Additionally, as regards v_z, the random forces of the thermal fluctuation are symmetrical in the z direction and the effect of the random force is cancelled. As a result, the thermal motion has negligible effects on the v_z obtained from the simulations in Fig. 3(a), thus yielding two peaks similar to those predicted by theory.

In general, Fig. 3 exhibits agreement between the theory and simulations, with this agreement being obtained by correction for the presence of the thermal fluctuation. However, the theory and simulations do not always agree in terms of Ω. In other words, the water nanotrain concept proposed based on the above phenomenological theory can be disturbed by such random forces. Therefore, we analyze our simulation data carefully in order to identify the specific frequency region in which the water nanotrain concept is viable.

Water nanotrain motion is found to occur at ω values of 0.625–25 THz (i.e., the shaded region in Fig. 3). In this frequency region, the water molecules exhibit a combination of linear propagation and unidirectional rotation, rather than the random flip-flop reorientation typically exhibited by water in carbon nanotubes [54, 55]. As an example, please see the "movie-1.avi" movie file in the supplementary material, which shows an example of the water nanotrain motion in the 12.5 THz field. In this case, when the linear transport of the water reaches a maximum $v_{z,max}$ (see Fig. 3), the water molecules also undergo the most regular rotation. In particular, we find that $v_{z,max}$ reaches a value of 1080 m/s in this case, which is higher than all the values reported

in the literature (e.g., Refs. [1, 7, 14, 21, 22, 25, 27, 29]). Furthermore, when the water molecules undergo the train-wheel-like motion within certain translational electric fields, both v_z and Ω are almost constant. The linear propagation and rotation of the water molecules are almost uniform. This coincides with our phenomenological assumptions in the theoretical analysis, i.e., that $\boldsymbol{F}_f$ in the z direction is closely related to v_z and Ω. In fact, the relation between the interfacial friction and water velocity is more complex when the water velocity is relatively high [56].

In addition, we analyze ω values lower than 0.625 THz, finding that the relevant motion is quite different to the train-wheel-like motion discussed above. As an example, please see the "movie-2.avi" movie file in the supplementary material, which was recorded at 0.568 THz. Such ω values correspond to a phase-propagation motion, because of the restriction of the phase velocities of the translational z-directed $\boldsymbol{E}$ [25]. In addition, we also investigate those ω larger than 25 THz, and observe that the corresponding motion is also distinct from the train-wheel-like motion. For instance, see the "movie-3.avi" movie file in the supplementary material, which was recorded at 62.5 THz. At such ω, no (average linear) transportation occurs, because the frequencies are too large for the water molecules to follow the translation of the z-directed electric field.

Figure 4(a) shows the simulation results for a series of higher-density systems that were obtained by adding more water molecules to our systems. This figure indicates that a higher water-molecule density corresponds to smaller v_z. A higher density leads to smaller gaps between the water molecules, so that the resultant stronger water electrostatic interactions (i.e., hydrogen bonds and Coulomb potentials) also act on the water dipole

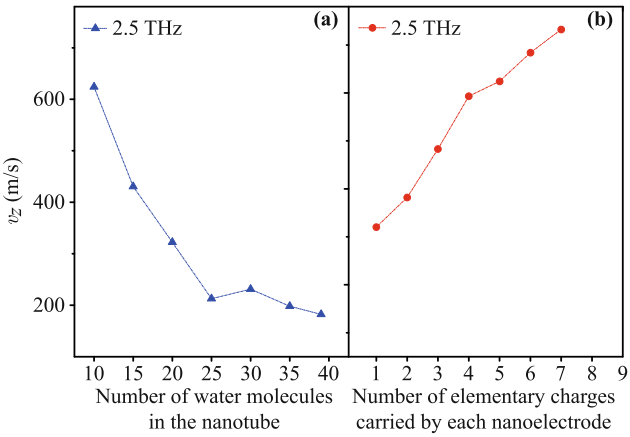

Fig. 4 **(a)** The relationship between the linear speed v_z and the number of the water molecules in the nanotube at 2.50 THz. **(b)** The relationship between the linear speed v_z and the number of elementary charges carried by each nanoelectrode at 2.50 THz.

orientations [52]. As the coupling between the water and the field is disturbed, the influence of the transport on the water declines. Figure 4(b) shows the simulation results for a series of systems in which the nanoelectrodes have a different number of elementary charges at 2.5 THz. Therefore, this simulation examines the effect of electric fields of various magnitudes on the transport. It is apparent that v_z increases with increased $\boldsymbol{E}$ magnitude, as expected from Eq. (8).

4 Conclusion and discussion

By developing the phenomenological Debye double-relaxation theory and performing independent molecular dynamics simulations, we have revealed an unprecedentedly fast unidirectional flow of single-file water molecules within a nanochannel in a model system. This approach was inspired by both biological (*the function of charge groups in biological membrane proteins is vital to water permeation through aquaporins*) and physical implications (*environmental oscillations arising from thermal motion occur when water molecules are transported through nanochannels*). Interestingly, we have found that the water molecules exhibit a train-wheel-like motion, i.e., a combination of both translational and rotational motion; we have labeled this behavior a *water nanotrain*. The underlying mechanism originates from the resonant relaxation dynamics of the H and O atoms.

The flow speed obtained in this work can be further increased by applying stronger fields in an appropriate manner. Also, the water-train water molecules (the angular speed of which can be controlled) may be potential substitutes for fullerene wheels in smaller nanocar designs [57]. A future experimental demonstration of this work could be performed using a carbon-nanotube nanochannel or other types of nanochannels or nanopores (which may even have a larger radius to allow a greater number of water molecules to be transported side-by-side). Besides water molecules, the present investigation could also be extended to treat other polar nanoparticles, such as proteins or DNA segments [58]. Furthermore, as molecular polarizability plays a crucial role in transportation, as revealed in this work, our method has an advantage in that selective transportation is achieved. In other words, the separation of polar molecules from nonpolar molecules, or polar molecules from other molecules with different polar properties, can be achieved. To summarize, the findings of this work have implications for nanotechnology, as regards the design of high-efficiency nanochannels or smaller nanodevices such as nanocars. These findings are also helpful for understanding and

controlling water flow across biological nanochannels in biology-related research.

Movie captions

All the movies are based on the simulation results. More details are presented in the article.

Movie 1. Train-wheel-like motion for water molecules at 12.5 THz.

Movie 2. Phase-propagation motion for water molecules at 0.568 THz.

Movie 3. No linear transport occurs at 62.5 THz. Note that the water molecules are still affected by the applied field and experience regular oscillation.

Acknowledgements We acknowledge the financial support by the National Natural Science Foundation of China under Grant No. 11222544, the Fok Ying Tung Education Foundation under Grant No. 131008, and the Program for New Century Excellent Talents in University (NCET-12-0121). The computational resources utilized in this research were provided by Shanghai Supercomputer Center.

References

1. T. B. Sisan and S. Lichter, Solitons transport water through narrow carbon nanotubes, *Phys. Rev. Lett.* 112(4), 044501 (2014)
2. C. B. Picallo, S. Gravelle, L. Joly, E. Charlaix, and L. Bocquet, Nanofluidic osmotic diodes: Theory and molecular dynamics simulations, *Phys. Rev. Lett.* 111(24), 244501 (2013)
3. K. Hata, D. N. Futaba, K. Mizuno, T. Namai, M. Yumura, and S. Iijima, Water-assisted highly efficient synthesis of impurity-free single-waited carbon nanotubes, *Science* 306(5700), 1362 (2004)
4. M. A. Shannon, P. W. Bohn, M. Elimelech, J. G. Georgiadis, B. J. Marinas, and A. M. Mayes, Science and technology for water purification in the coming decades, *Nature* 452(7185), 301 (2008)
5. A. Srivastava, O. N. Srivastava, S. Talapatra, R. Vajtai, and P. M. Ajayan, Carbon nanotube filters, *Nat. Mater.* 3(9), 610 (2004)
6. Y. B. Chen, Y. H. Liu, Y. Zeng, W. Mao, L. Hu, Z. L. Mao, and H. Q. Xu, Optimal aspect ratio of endocytosed spherocylindrical nanoparticle, *Front. Phys.* 10(1), 116 (2015)
7. C. Lee, C. Cottin-Bizonne, A. L. Biance, P. Joseph, L. Bocquet, and C. Ybert, Osmotic flow through fully permeable nanochannels, *Phys. Rev. Lett.* 112(24), 244501 (2014)
8. G. Hummer, J. C. Rasaiah, and J. P. Noworyta, Water conduction through the hydrophobic channel of a carbon nanotube, *Nature* 414(6860), 188 (2001)
9. X. J. Gong, J. Y. Li, H. Zhang, R. Z. Wan, H. J. Lu, S. Wang, and H. P. Fang, Enhancement of water permeation across a nanochannel by the structure outside the channel, *Phys. Rev. Lett.* 101(25), 257801 (2008)
10. X. J. Gong, J. Y. Li, H. J. Lu, R. Z. Wan, J. C. Li, J. Hu, and H. P. Fang, A charge-driven molecular water pump, *Nat. Nanotechnol.* 2(11), 709 (2007)
11. M. Ma, F. Grey, L. M. Shen, M. Urbakh, S. Wu, J. Z. Liu, Y. L. Liu, and Q. S. Zheng, Water transport inside carbon nanotubes mediated by phonon-induced oscillating friction, *Nat. Nanotechnol.* 10(8), 692 (2015)
12. Y. L. Zhao, Y. L. Song, W. G. Song, W. Liang, X. Y. Jiang, Z. Y. Tang, H. X. Xu, Z. X. Wei, Y. Q. Liu, M. H. Liu, L. Jiang, X. H. Bao, L. J. Wan, and C. L. Bai, Progress of nanoscience in China, *Front. Phys.* 9(3), 257 (2014)
13. G. X. Guo, L. Zhang, and Y. Zhang, Molecular dynamics study of the infiltration of lipid-wrapping C60 and polyhydroxylated single-walled nanotubes into lipid bilayers, *Front. Phys.* 10(2), 177 (2015)
14. M. Majumder, N. Chopra, R. Andrews, and B. J. Hinds, Nanoscale hydrodynamics - enhanced flow in carbon nanotubes, *Nature* 438(7064), 44 (2005)
15. J. K. Holt, H. G. Park, Y. M. Wang, M. Stadermann, A. B. Artyukhin, C. P. Grigoropoulos, A. Noy, and O. Bakajin, Fast mass transport through sub-2-nanometer carbon nanotubes, *Science* 312(5776), 1034 (2006)
16. J. A. Thomas and A. J. H. McGaughey, Water flow in carbon nanotubes: Transition to subcontinuum transport, *Phys. Rev. Lett.* 102(18), 184502 (2009)
17. C. Lee, C. Cottin-Bizonne, A. L. Biance, P. Joseph, L. Bocquet, and C. Ybert, Osmotic flow through fully permeable nanochannels, *Phys. Rev. Lett.* 112(24), 244501 (2014)
18. A. Kalra, S. Garde, and G. Hummer, Osmotic water transport through carbon nanotube membranes, *Proc. Natl. Acad. Sci. USA* 100(18), 10175 (2003)
19. A. Ajdari and L. Bocquet, Giant amplification of interfacially driven transport by hydrodynamic slip: Diffusio-osmosis and beyond, *Phys. Rev. Lett.* 96(18), 186102 (2006)
20. M. J. Longhurst and N. Quirke, Temperature-driven pumping of fluid through single-walled carbon nanotubes, *Nano Lett.* 7(11), 3324 (2007)
21. Q. L. Zhang, W. Z. Jiang, J. Liu, R. D. Miao, and N. Sheng, Water transport through carbon nanotubes with the radial breathing mode, *Phys. Rev. Lett.* 110(25), 254501 (2013)
22. Y. Wang, Y. J. Zhao, and J. P. Huang, Giant pumping of single-file water molecules in a carbon nanotube, *J. Phys. Chem. B* 115(45), 13275 (2011)
23. X. W. Meng, Y. Wang, Y. J. Zhao, and J. P. Huang, Gating of a water nanochannel driven by dipolar molecules, *J. Phys. Chem. B* 115(16), 4768 (2011)
24. Z. Chi, C. Luo, and Y. Dai, Comment on "Electrical-driven transport of endohedral fullerene encapsulating a single water molecule, *Phys. Rev. Lett.* 113(11), 119601 (2014)
25. K. F. Rinne, S. Gekle, D. J. Bonthuis, and R. R. Netz, Nanoscale pumping of water by AC electric fields, *Nano Lett.* 12(4), 1780 (2012)
26. S. de Luca, B. D. Todd, J. S. Hansen, and P. J. Daivis, Electropumping of water with rotating electric fields, *J. Chem. Phys.* 138(15), 154712 (2013)

27. X. P. Li, G. P. Kong, X. Zhang, and G. W. He, Pumping of water through carbon nanotubes by rotating electric field and rotating magnetic field, *Appl. Phys. Lett.* 103(14), 143117 (2013)
28. J. Wong-ekkabut, M. S. Miettinen, C. Dias, and M. Karttunen, Static charges cannot drive a continuous flow of water molecules through a carbon nanotube, *Nat. Nanotechnol.* 5(8), 555 (2010)
29. J. Su and H. X. Guo, Control of unidirectional transport of single-file water molecules through carbon nanotubes in an electric field, *ACS Nano* 5(1), 351 (2011)
30. M. O. Jensen, E. Tajkhorshid, and K. Schulten, Electrostatic tuning of permeation and selectivity in aquaporin water channels, *Biophys. J.* 85(5), 2884 (2003)
31. E. Tajkhorshid, P. Nollert, M. O. Jensen, L. J. W. Miercke, J. O'Connell, R. M. Stroud, and K. Schulten, Control of the selectivity of the aquaporin water channel family by global orientational tuning, *Science* 296(5567), 525 (2002)
32. B. L. de Groot, T. Frigato, V. Helms, and H. Grubmuller, The mechanism of proton exclusion in the aquaporin-1 water channel, *J. Mol. Biol.* 333(2), 279 (2003)
33. J. S. Hub and B. L. de Groot, Mechanism of selectivity in aquaporins and aquaglyceroporins, *Proc. Natl. Acad. Sci. USA* 105(4), 1198 (2008)
34. B. L. de Groot and H. Grubmuller, Water permeation across biological membranes: Mechanism and dynamics of aquaporin-1 and GlpF, *Science* 294(5550), 2353 (2001)
35. J. P. Huang, K. W. Yu, and G. Q. Gu, Electrorotation of a pair of spherical particles, *Phys. Rev. E* 65(2), 021401 (2002)
36. J. P. Huang, M. Karttunen, K. W. Yu, and L. Dong, Dielectrophoresis of charged colloidal suspensions, *Phys. Rev. E* 67(2), 021403 (2003)
37. T. Meissner and F. J. Wentz, IEEE transactions on geoscience and remote sensing, *Complex Dielectric Constant of Pure and Sea Water from Microwave Satellite Observations* 42(9), 1836 (2004)
38. J. P. Huang and K. W. Yu, Enhanced nonlinear optical responses of materials: Composite effects, *Phys. Rep.* 431(3), 87 (2006)
39. G. Chen, P. Tan, S. Chen, J. P. Huang, W. Wen, and L. Xu, Coalescence of pickering emulsion droplets induced by an electric field, *Phys. Rev. Lett.* 110(6), 064502 (2013)
40. P. Debye, Polar Molecules, Chemical Catalog Company, New York, 1929
41. J. T. Kindt and C. A. Schmuttenmaer, Far-infrared dielectric properties of polar liquids probed by femtosecond terahertz pulse spectroscopy, *J. Phys. Chem.* 100(24), 10373 (1996)
42. C. Ro?nne, L. Thrane, P.O. Åstrand, A. Wallqvist, K. V. Mikkelsen, and S. R. Keiding, Investigation of the temperature dependence of dielectric relaxation in liquid water by THz reflection spectroscopy and molecular dynamics simulation, *J. Phys. Chem.* 107(14), 5319 (1997)
43. H. J. Liebe, G. A. Hufford, and T. Manabe, A model for the complex permittivity of water at frequencies below 1 THz, *J. Infrared Millim. Terahertz Waves* 12(7), 659 (1991)
44. R. Buchner, J. Barthel, and J. Stauber, The dielectric relaxation of water between 0 ^{o}C and 35 ^{o}C, *Chem. Phys. Lett.* 306(1-2), 57 (1999)
45. Y. Huang, X. B. Wang, J. A. Tame, and R. Pethig, Electrokinetic behaviour of colloidal particles in travelling electric fields: Studies using yeast cells, *J. Phys. D Appl. Phys.* 26(9), 1528 (1993)
46. S. Fiedler, S. G. Shirley, T. Schnelle, and G. Fuhr, G, Dielectrophoretic sorting of particles and cells in a microsystem, *Anal. Chem.* 70(9), 1909 (1998)
47. M. S. Talary, J. P. H. Burt, J. A. Tame, and R. Pethig, Electromanipulation and separation of cells using travelling electric fields, *J. Phys. D Appl. Phys.* 29(8), 2198 (1996)
48. U. Zimmermann, Electric field-mediated fusion and related electrical phenomena, *Biochim. Biophys. Acta* 694(3), 227 (1982)
49. K. Falk, F. Sedlmeier, L. Joly, R. R. Netz, and L. Bocquet, Molecular origin of fast water transport in carbon nanotube membranes: Superlubricity versus curvature dependent friction, *Nano Lett.* 10(10), 4067 (2010)
50. B. Hess, et al., Gromacs-3.3, Department of Biophysical Chemistry, University of Groningen, Groningen, 2005
51. W. L. Jorgensen, J. Chandrasekhar, J. D. Madura, R. W. Impey, and M. L. Klein, Comparison of simple potential functions for simulating liquid water, *J. Chem. Phys.* 79(2), 926 (1983)
52. B. Mukherjee, P. K. Maiti, C. Dasgupta, and A. K. Sood, Strongly anisotropic orientational relaxation of water molecules in narrow carbon nanotubes and nanorings, *ACS Nano* 2(6), 1189 (2008)
53. A. B. Farimani, Y. Wu, and N. R. Aluru, Rotational motion of a singlewater molecule in a buckyball, *Phys. Chem. Chem. Phys.* 15(41), 17993 (2013)
54. J. Su and H. X. Guo, Control of unidirectional transport of single-file water molecules through carbon nanotubes in an electric field, *ACS Nano* 5(1), 351 (2011)
55. H. P. Fang, R. Z. Wan, X. J. Gong, H. J. Lu, and S. Y. Li, Dynamics of single-file water chains inside nanoscale channels: physics, biological significance and applications, *J. Phys. D* 41(10), 103002 (2008)
56. M. D. Ma, L. M. Shen, J. Sheridan, J. Z. Liu, C. Chen, and Q. S. Zheng, Friction of water slipping in carbon nanotubes, *Phys. Rev. E* 83(3), 036316 (2011)
57. T. Kudernac, N. Ruangsupapichat, M. Parschau, B. Macia, N. Katsonis, S. R. Harutyunyan, K. H. Ernst, and B. L. Feringa, Electrically driven directional motion of a four-wheeled molecule on a metal surface, *Nature* 479(7372), 208 (2011)
58. E. W. Frey, A. A. Gooding, S. Wijeratne, and C. H. Kiang, Understanding the physics of DNA using nanoscale single-molecule manipulation, *Front. Phys.* 7(5), 576 (2012)